Dalton Transactions

Cite this: *Dalton Trans.*, 2011, **40**, 393

www.rsc.org/dalton

PAPER

Octathienyl/phenyl-substituted zinc phthalocyanines J-aggregated through conformational planarization†

Zihui Chen,*[a,b] Lihong Niu,[a] Yuanhua Cheng,[a] Xinyu Zhou,[a] Cheng Zhong[a] and Fushi Zhang*[a]

Received 19th August 2010, Accepted 6th October 2010
DOI: 10.1039/c0dt01066a

A novel family of thiophene-decorated phthalocyanines (M-TPcs) was efficiently synthesized, during which the key intermediate of these compounds was purified through a chemical approach. In the optimized geometries of M-TPcs, the peripherally linked thiophene rings are tilted from the Pc core, which oppose aggregation considering the mutual steric hindrance. However, Zn-TPc formed J-aggregates in many solvents while Ni-TPc and Cu-TPc did not. Octaphenyl-substituted zinc Pc (Zn-PPc) showed similar J-aggregation behavior as Zn-TPc. This unusual J-aggregation was attributed to the conformational planarization of the corresponding molecules.

Introduction

Being a versatile class of functional dyes, the importance and potential of phthalocyanines (Pcs) are rapidly growing in modern science. This is mainly because of their high degree of aromaticity, their intriguing electronic and optical characteristics, their exceptionally high chemical and thermal stability, and the flexibility involved in the synthesis of these compounds.[1] Moreover, different metal atoms in the center and substituents on the sides of the large Pc ring endow Pcs with various functionalities. Synthetic chemists are able to rationally design the structure of Pc according to their own needs.[2]

It has been well-established that Pcs can form two types of one-dimensional aggregates, namely face-to-face H-aggregates and head-to-tail J-aggregates.[3] The J-aggregated Pcs are characterized by a remarkable bathochromic shift of the Q-band absorption, whereas the H-aggregated counterparts show a hypsochromic shift from the isolated monomers. Pcs form preferentially the H-aggregates, but J-aggregates are promising for various technological applications such as spectral sensitization, optical storage, and nonlinear optics.[4] In light of such considerations, it is not surprising that methods to assemble J-aggregates of Pcs are being actively pursued. To date, most reported J-aggregates of Pc were achieved either by utilizing the coordination of the side substituent from one Pc molecule to the central metal ion in a neighbor,[5] or by interfacial engineering.[6] Isago[7] reported a novel antimony(III)-Pc complex that could J-aggregate in dichloromethane. However, the J-aggregation mechanism of this compound is as yet unknown.

During our exploration of photo-controllable self-assemblies of functional dyes, we synthesized a novel family of thiophene-decorated Pcs, namely 2,3,9,10,16,17,24,25-octakis(2,5-dimethyl-3-thienyl) metal Pcs (abbreviated as M-TPc), and unexpectedly discovered that Zn-TPc was able to J-aggregate in many solvents in an unprecedented manner.

Besides the intriguing J-aggregation behavior, M-TPcs may exhibit some other unusual physicochemical properties, considering the unique optical and redox properties of thiophene rings, as well as their self-assembly properties on solid surfaces or in the bulk.[8] The high polarizability of the sulfur atom in thiophene ring leads to a low aromatic stabilization energy, which is the most important reason for it being widely used as constructing units of many functional materials, such as charge-transporting molecules[9] and thermally irreversible photochromic compounds.[10] In addition, the non-bonding sulfur–sulfur interaction of neighboring thiophenes is also very interesting to scientists.[11] Tian and co-workers designed a series of bis-thienylethene-based tetraazoporphyrin and Pc hybrids as photo-switching molecules.[12] These thiophene-Pc hybrids showed photochromism in chloroform and the fluorescence intensity of these compounds could be photo-regulated. It is well-known that the unique physico-chemical properties of Pcs generally arise from their large flat aromatic surface. Any change to this surface can exert unpredictable influences on the special electronic and optical properties of Pcs, as well as their

[a]*The Key Lab of Organic Photoelectrons & Molecular Engineering of Ministry of Education, Department of Chemistry, Tsinghua University, Beijing, 100084, PR China*
[b]*Department of Physics & Tsinghua-Foxconn Nanotechnology Research Centre, Tsinghua University, Beijing, China. E-mail: zhchen@tsinghua.edu.cn, zhangfs@tsinghua.edu.cn; Fax: + 86 10 62770304; Tel: +86 10 62782596*

† Electronic supplementary information (ESI) available: Fig. S1: (a) The TLC experiment of intermediate **2** and the product obtained from the Suzuki cross-coupling reaction, with a 2 : 1 mixed solvent of petroleum ether and ethyl acetate as eluent. (b) ^{1}H NMR spectra of the product in $CDCl_3$. Fig. S2: TLC experiments in the synthesis of phthalonitrile **7** from the mixture obtained from the Suzuki cross-coupling reaction. Fig. S3: UV-Vis spectrum of Cu-TPc and Ni-TPc in THF ($c = 1 \times 10^{-4}$ mol L^{-1}). Fig. S4: ^{1}H NMR spectra of Ni-TPc and Zn-TPc. Fig. S5: UV-Vis spectrum of Zn-TPc in THF ($c = 2 \times 10^{-5}$ mol L^{-1}). Fig. S6: UV-Vis spectral changes of Zn-TPc ($c = 2 \times 10^{-5}$ mol L^{-1}) in chloroform upon the addition of a drop of pyridine. Fig. S7: Plot of $\lg(c - (A_{700}/\varepsilon_{700}))$ *vs.* $\lg(A_{700}/\varepsilon_{700})$ of Zn-TPc in the concentration range of 1.25×10^{-6} to 2×10^{-5} mol L^{-1}. Fig. S8: Computer optimized conformation of Zn-PPc by energy minimization method. See DOI: 10.1039/c0dt01066a

self-assembly behavior. Therefore, thiophene-decorated Pc in which the basic skeleton of Pc is kept intact, may be a better prototype to combine the respective advantages of thiophenes and Pc than corresponding hybrids. However, such compounds are as yet rarely reported. Muto *et al.*[13] first prepared a Pc derivative bearing eight 2-thienyl substituents at the β-postions. By electrochemical oxidation of this Pc, they constructed a π-conjugated polymer film which has potential electrochromic material applications.

Taking into account all the significant factors mentioned above, we report here the synthesis and J-aggregation properties of M-TPcs with specific discussion on the possible J-aggregation mechanism.

Results and discussion

Synthesis

As shown in Scheme 1, the synthesis of M-TPcs started with the Suzuki cross-coupling of 2,5-dimethylthien-3-ylboronic acid with 4,5-dibromophthalic acid dimethyl ester in the presence of $Pd(PPh_3)_4$ to give the key intermediate **2**. However, coupling of the second equivalent of boronic acid was proven to be inefficient

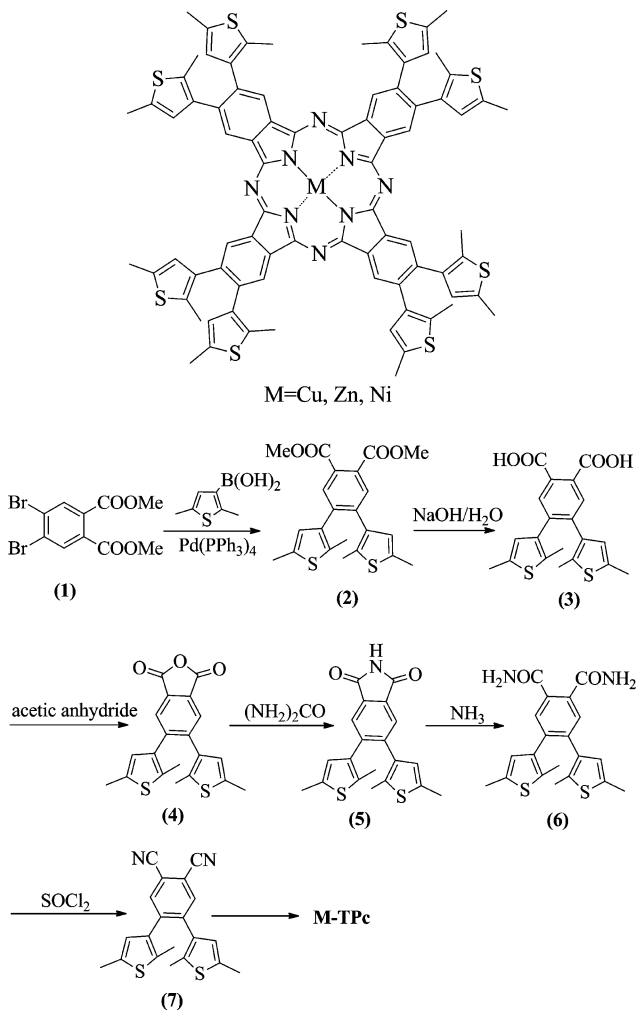

Scheme 1 The structures and synthetic route for Cu-TPc, Zn-TPc and Ni-TPc.

even after prolonged reaction time, probably as a result of the steric bulkiness of the system.[14] To make matters worse, the R_f value of the product is exactly the same as that of reagent **1**, which means that complete purification of compound **2** by chromatography is probably very difficult. Column chromatography on silica gel with petroleum–ethyl acetate (5 : 1, volume ratio) afforded a mixture containing compound **2** as a yellow ropy liquid, and ^{1}H NMR experiments showed that the mixture was composed of reagent **1**, intermediate **2** and the mono-substituted byproduct **8** with a molar ratio of about 1 : 1.75 : 1 (Fig. S1, ESI†). These results apparently ruled out recrystallization as an alternative method for the purification of compound **2**.

Since the products obtained from Suzuki cross-coupling reaction cannot be purified directly with simple physical methods, the exploration of effective chemical approaches in purification of intermediate **2** is of vital importance to the synthetic route in Scheme 1.

According to our experience, the reactions involved in the synthesis of phthalonitrile **7** from compound **2** are very reliable (Scheme 1) with conversions close to quantitative. Besides, the molecular polarity of desired product is quite different from that of reagents in each step, which is excellent for purification. With the synthesis route discussed above, compounds **8** and **1** were converted to the corresponding phthalonitriles **9** and **10** (structures shown in Scheme 2). Note that the bromo-groups in these compounds are extremely mobile leaving groups in S_NAr reactions and thus, can be substituted with various nucleophiles. Based on this observation, a cascade synthetic strategy of M-TPcs was designed.

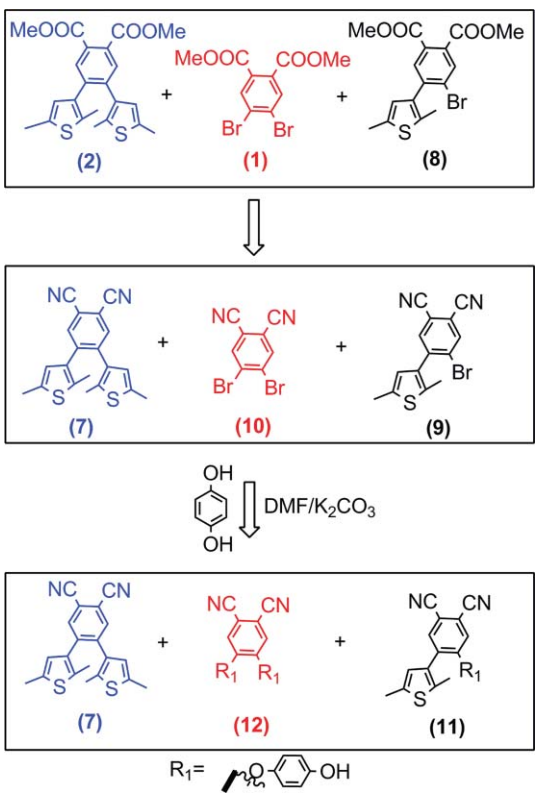

Scheme 2 The synthesis and purification of intermediate **7**.

The mixture obtained from the Suzuki cross-coupling reaction was directly used for the preparation of phthalonitrile **7** according to predetermined route in Scheme 1. For each step in this route, only TLC was employed to monitor the synthesis process (Fig. S2, ESI†). The crude products obtained were used directly in the next steps without purification. As shown in Scheme 2, after compounds **1**/**2**/**8** were converted to corresponding phthalonitriles, the resulting mixtures were treated with an excess of hydroquinone and K_2CO_3 in *N*,*N*-dimethylformamide (DMF) at room temperature. Phthalonitriles **9** and **10** transformed to compound **11** and **12** completely, while phthalonitrile **7** remained unchanged. Compounds **11** and **12** could then react with sodium hydroxide to form water-soluble compounds. Therefore, a mixture of compounds **11**, **12** and **7** was added to an aqueous solution of sodium hydroxide. After stirring for a few minutes, the insoluble substance was mostly phthalonitrile **7**. Further purification with column chromatography over silica gel produced pure phthalonitrile **7** with a total yield of 19%.

Having completed the preparation of intermediate **7**, we now intended to complete the synthesis of M-TPcs. A mixture of phthalonitrile **7** and salts of appropriate metals in ethoxyethanol were refluxed for 3 h under nitrogen to yield the target products Cu-TPc, Zn-TPc and Ni-TPc. These products were characterized by IR, MS, UV-Vis spectroscopy and elemental analysis.

Aggregation abilities

Typical UV-Vis spectra of monomeric Pcs feature two distinct absorption bands, namely the B- and Q-band, which can be readily interpreted by using of Gouterman's highly simplified four-orbital model.[15] The UV-Vis spectra of Cu-TPc and Ni-TPc in tetrahydrofuran (THF) are depicted in Fig. 1. Both of the samples showed sharp, intense Q bands, which were at 694 nm (Cu-TPc) and 692 nm (Ni-TPc), respectively. The absorptions of these complexes obey the Beer–Lambert law in a concentration range from 1.25×10^{-6} to 1×10^{-4} mol L^{-1} (Fig. S3, ESI†). The UV-Vis absorption properties of Cu-TPc and Ni–Pc in chloroform, toluene and DMSO were quite similar to those in THF, suggesting that these two Pcs were essentially evenly dispersed in these solvents.

The excellent dispersibility of Ni-TPc was further demonstrated by ^{1}H NMR (Fig. S4A, ESI†). The resonance signals of Ni-TPc in *d*-chloroform ($c = 1.5 \times 10^{-3}$ mol L^{-1}) are well defined. The hydrogens atom on the benzene ring is located at 9.29 ppm and that on the thiophene ring is located at 6.69 ppm. These single peaks are well consistent with the symmetrical structure of Ni-TPc, indicating that this compound exists as monomers in chloroform even at such high concentration.

Zn-TPc showed very different UV-Vis absorption behavior. Fig. 2 displays the concentration-dependent UV-Vis spectra of Zn-TPc in THF. It can be seen that in this concentration range, Zn-TPc exhibited typical monomeric absorption behavior, which suggested a homogeneous dispersion in solution. However, when the concentration of Zn-TPc exceeded 2×10^{-5} mol L^{-1}, in addition to the normal Q-band at 694 nm, a red-shifted band at 740 nm was observed (Fig. S5, ESI†).

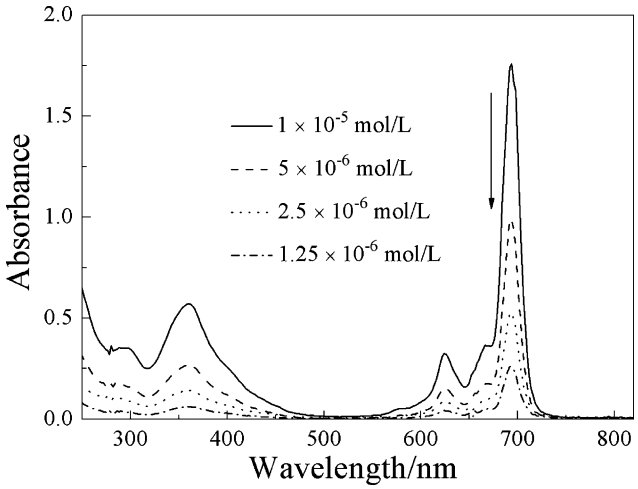

Fig. 2 Concentration-dependent UV-Vis spectra of Zn-TPc in THF.

This unusual red-shifted band was much more remarkable in chloroform. As shown in Fig. 3, in addition to the typical Q-absorption at 700 nm, the absorption of Zn-TPc in chloroform exhibited a broad red-shifted band at 750 nm. After adding small amounts of ethyl acetate (EA) to the chloroform solution

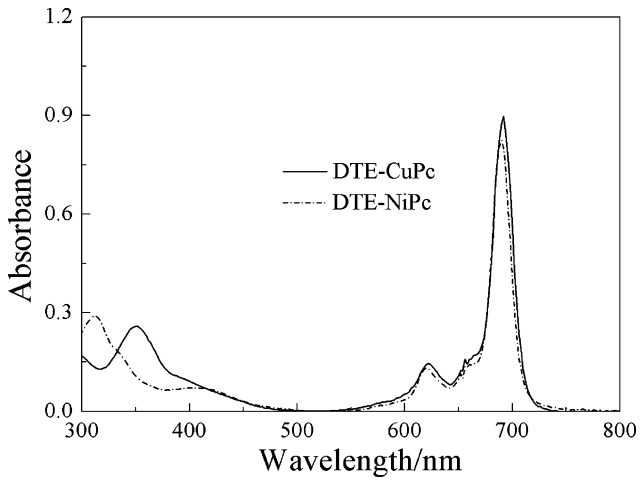

Fig. 1 UV-Vis spectra of Cu-TPc and Ni-TPc in THF ($c = 5 \times 10^{-6}$ mol L^{-1}).

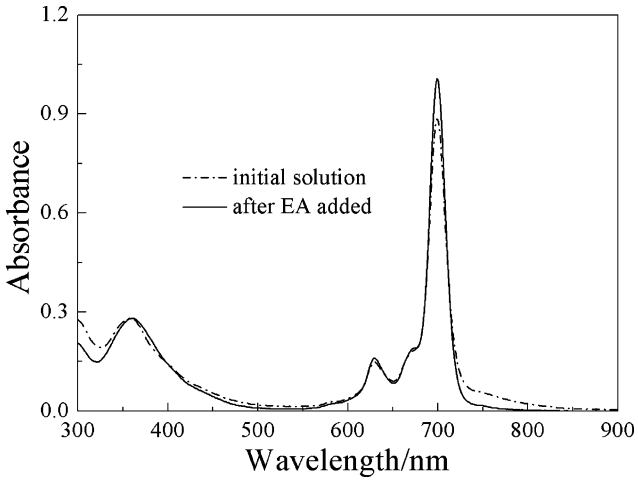

Fig. 3 UV-Vis spectra of Zn-TPc in chloroform (---) and in a 20 : 1 mixed solvent of chloroform and EA (—); $c = 5 \times 10^{-6}$ mol L^{-1}.

of Zn-TPc, the absorbance at 700 nm increased from 0.89 to 1.01, whereas the red-shifted peak at 750 nm disappeared. As a consequence, a typical monomeric spectrum was obtained. It was noted that some other solvents such as pyridine and DMF show a similar but more effective role relative to that of EA (Fig. S6, ESI†).

Generally, there are three possibilities that can produce the unusual red-shifted absorption in Fig. 3: (1) oxidation of Pc ring; (2) monoprotonation of Pc ring; (3) J-aggregation of Pc molecules. The first possibility can be readily ruled out by the lack of the typical broad absorption of an oxidized Pc ring in the region of 520 nm. Aforementioned titration experiments can also rule out the oxidation mechanism since EA, pyridine and DMF are all far from good reductants. Moreover, compared with the basic nitrogen atoms in the Pc ring, EA is a much weaker proton acceptor. It is unlikely therefore that EA can deprotonate the protonated Pc molecules. Therefore, the spectral changes of Zn-TPc in chloroform upon the addition of EA also make the second possibility unlikely.

To thoroughly rule out the second possibility, a study of the UV-Vis spectra of monoprotonated Zn-TPc is helpful. The monoprotonation of Pc ring was achieved by adding trifluoroacetic acid (TFA) to a 20 : 1 chloroform–EA solution of Zn-TPc. As shown in Fig. 4, with increasing TFA concentration, the absorption at 700 nm decreased sharply, while a new red-shifted absorption band at 746 nm emerged with four isobestic points at 329, 408, 571 and 720 nm. The intensity of this new band at 746 nm reached its maximum when the TFA concentration exceeded 0.45 mol L^{-1}; use of an excess of TFA resulted in the degradation of Zn-TPc. Compared with Fig. 3, not only the shape of the red-shifted Q-band, but also the positions of isobestic points shown in Fig. 4 were apparently different, suggesting that the red-shifted absorption of Zn-TPc in chloroform was not originated from protonation.

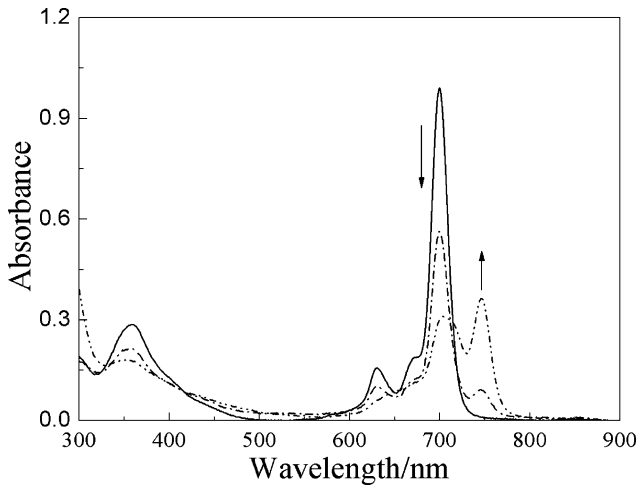

Fig. 4 Absorption spectral changes upon the addition of TFA to Zn-TPc (5×10^{-6} mol L^{-1}) in 20 : 1 mixed solvent of chloroform and EA.

Therefore it seems that the unusual red-shifted band of Zn-TPc in Fig. 3 might be attributed to the formation of Pc J-aggregates. This assumption was first demonstrated by the concentration-dependent UV-Vis spectra of Zn-TPc in chloroform and further corroborated with fluorescence spectra.

The concentration-dependent absorptions of Zn-TPc in chloroform are shown in Fig. 5. With an increase in concentration, the apparent molar extinction coefficient at 700 nm became smaller. In turn, the intensity of the band around 750 nm grew. In a solid film, the relative intensity of the lower energy band became comparable to that of the higher energy counterpart. These concentration-dependent spectral changes of Zn-TPc are typical of molecular J-aggregation in an equilibrium process.

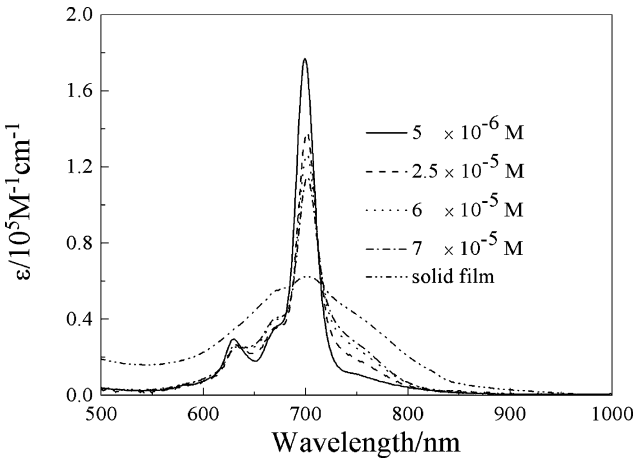

Fig. 5 Concentration dependent UV-Vis spectra (in Q-region) of Zn-TPc in chloroform.

It is well known that the efficiencies of processes such as energy transfer and electron transfer are sensitive to the aggregation state of dyes,[16] and the formation of J-aggregates often lead to a decrease of fluorescence yield of Pcs. Fig. 6 showed the fluorescence emission spectra of Zn-TPc in THF and chloroform when excited at 650 nm. Compared with that in THF, the fluorescence quantum yield of Zn-TPc in chloroform was decreased from 0.21 to 0.09. Together with above-discussed UV-Vis absorption studies, the different fluorescence spectra of Zn-TPc in different solvents can simply be ascribed to that Zn-TPc showed a stronger tendency to J-aggregate in chloroform than in THF.

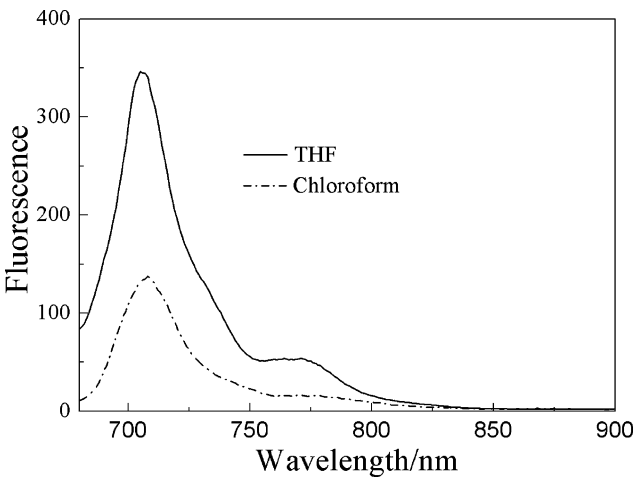

Fig. 6 Fluorescence spectra of Zn-TPc in THF and chloroform when excited at 650 nm ($c = 5 \times 10^{-6}$ mol L^{-1}).

^{1}H NMR experiments provided another powerful line of evidence for the J-aggregation of Zn-TPc. In a 5 : 1 mixed solvent of *d*-chloroform and d_5-pyridine, as shown in Fig. 7(a), the resonance signals of Zn-TPc ($c = 1.5 \times 10^{-3}$ mol L^{-1}) are well-defined (the peaks at 8.62, 7.65, 7.55 and 7.26 ppm are ascribed to the solvents (Fig. S4C, ESI†)). The single peak at 9.53 ppm belongs to the hydrogen atoms on the benzene rings. The hydrogen atoms on the thiophene rings showed a signal at 6.79 ppm. Additionally, there are two single peaks located at 2.51 and 2.37 ppm, respectively, which belong to the two types of methyl groups on the thiophene rings. The ratio of the integral areas of these four peaks is 1 : 1 : 3 : 3. All the ^{1}H NMR signals shown in Fig. 7(a) are consistent with the D_{4h} symmetrical structure of monomeric Zn-TPc, clearly demonstrating the purity of Zn-TPc. In *d*-chloroform ($c = 1.5 \times 10^{-3}$ mol L^{-1}), as shown in Fig. 7(b), the ^{1}H NMR spectrum of Zn-TPc became much more complex. Compared with Fig. 7(a), the intensity of the signal at 9.53 dropped significantly and the signal at 6.79 disappeared, accompanied by the appearance of more than eight new signals. When the concentration of Zn-TPc increased to 1.5×10^{-2} mol L^{-1}, the ^{1}H NMR spectrum of Zn-TPc was remarkably different from that at low concentration. As shown in Fig. 7(c), the resonance signals of Zn-TPc observed in Fig. 7(b) almost vanished, concomitant with the appearance of two new peaks at 6.98 and 5.01 ppm. These signals in Fig. 7(b) and 7(c) are no longer consistent with a D_{4h} symmetrical structure of Zn-TPc.

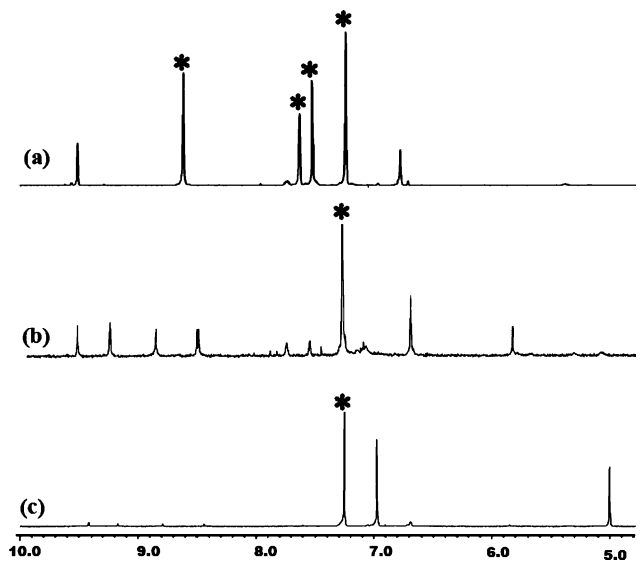

Fig. 7 ^{1}H NMR spectra of (a) 1.5×10^{-3} mol L^{-1} Zn-TPc solution in a 5 : 1 mixed solvent of *d*-chloroform and d_5-pyridine; (b) 1.5×10^{-3} mol L^{-1} Zn-TPc solution in *d*-chloroform; (c) 1.5×10^{-2} mol L^{-1} Zn-TPc solution in *d*-chloroform. The signals marked with asterisks are due to solvents.

Both the aggregation and monoprotonation of Pc ring could lower the symmetry of Zn-TPc. However, for a dynamic protonation–deprotonation equilibrium of Pcs, the variation in concentration can only change the relative intensity of signals but not their position. Therefore, the concentration-dependent ^{1}H NMR spectra of Zn-TPc in chloroform also have eliminated the possibility of a protonation mechanism. Besides, it was also observed that the relative integral areas of the signals in Fig. 7(b) and 7(c) deviated from theoretical values, which can be readily explained by the shielding effect of aggregation.

The average aggregation number (n) and the aggregation equilibrium constant (k) of Zn-TPc in chloroform can be estimated according to the following procedures. This procedure assumes single-step equilibrium between the monomers and the aggregate (eqn (1)):

$$n\,\mathrm{M} \rightleftharpoons \mathrm{M}_n \tag{1}$$

where M is the monomer of Zn-TPc, and M_n is the J-aggregate of Zn-TPc with aggregation number n.

Defining the overall concentration of Zn-TPc as c and the concentration of monomer is c_1 when the equilibrium is established, then the concentration of aggregates will be $(c - c_1)/n$ at equilibrium. Then, the aggregation equilibrium constant (k) is given by eqn (2):

$$k = (c - c_1)/nc_1^{\,n} \tag{2}$$

In our experiments, the Q-absorbance of momomeric phthalocyanine at a certain concentration is almost constant in different solvents, *e.g.* toluene, THF, *etc.* Then ε_{700} (the molar extinction coefficient of monomeric Zn-TPc at 700 nm) can be calculated from Fig. 3 to be 1.97×10^5, and A_{700} at different concentrations can be read from Fig. 5.

Then c_1 can be calculated by eqn (3):

$$A_{700}/\varepsilon_{700} \tag{3}$$

Based on eqn (2) and eqn (3), we obtain k from eqn (4):

$$k = \frac{c - (A_{700}/\varepsilon_{700})}{n(A_{700}/\varepsilon_{700})^n} \tag{4}$$

This can be rewritten as:

$$\lg(c - (A_{700}/\varepsilon_{700})) = \lg nk + n\lg(A_{700}/\varepsilon_{700}) \tag{5}$$

At fixed temperature, n, k and ε_{700} are constant. Therefore, if $\lg(c - (A_{700}/\varepsilon_{700}))$ is plotted against $\lg(A_{700}/\varepsilon_{700})$, a straight line should be obtained. The slope of this line is n and the intercept is at $\lg nk$.

Such a plot is shown in Fig. 8. Accordingly, we calculated $n = 1.78$ and $k = 1060$ when the concentration of Zn-TPc varied

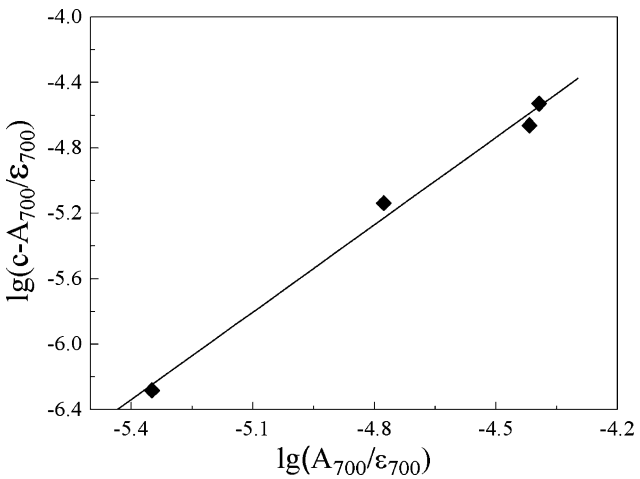

Fig. 8 Plot of $\lg(c - (A_{700}/\varepsilon_{700}))$ *vs.* $\lg(A_{700}/\varepsilon_{700})$ with the concentration of Zn-TPc varied from 5×10^{-6} to 7×10^{-5} mol L^{-1}.

from 5×10^{-6} to 7×10^{-5} mol L^{-1}. However, in the concentration range of 1.25×10^{-6} to 2×10^{-5} mol L^{-1}, n and k of Zn-TPc in chloroform were calculated as 1.10 and 2.32, respectively (Fig. S7, ESI†), which indicated that the concentration of Zn-TPc exerted significant influence on its aggregation behavior. The larger the concentration, the easier it is for Zn-TPc to aggregate.

Abaham *et al.*[17] reported Zn(II) porphyrins which could form aggregates in chloroform through a mechanism involving π–π stacking, and found that accompanying the aggregation, the ^{1}H NMR signals corresponding to the hydrogen atoms on the porphyrin ring were remarkably upfield shifted. From Fig. 7, it can be seen that Zn-TPc showed a similar tendency as those porphyrins. Therefore, we deduced that intermolecular π–π interaction also was the dominating driving force for the J-aggregation of Zn-TPc.

To test this assumption, we subsequently measured the UV-Vis spectrum of Zn-TPc in toluene. Unlike pyridine, toluene can not coordinate with ZnPc, however, it can disrupt the π–π interaction.[18] Therefore, if it is true that Zn-TPc underwent J-aggregation through intermolecular π–π stacking, the aggregation tendency of Zn-TPc in toluene will be weaker than that in chloroform. As shown in Fig. 9, the experimental result indeed matched the above prediction. For a 5×10^{-6} mol L^{-1} solution of Zn-TPc in toluene, the value of A_{700}/A_{750} in toluene is about 36, which is 2.3 times larger than that in chloroform.

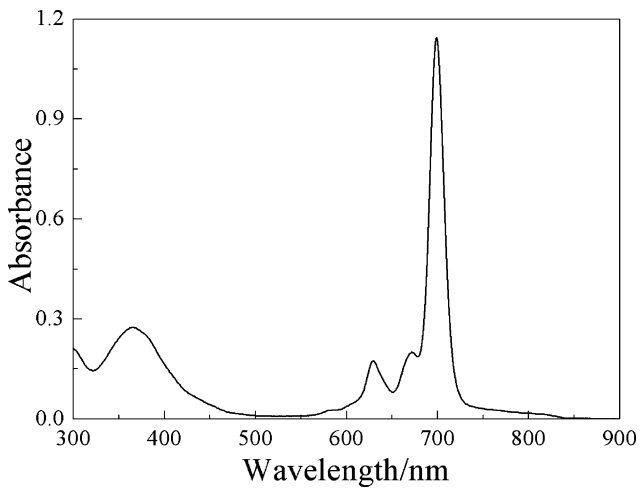

Fig. 9 UV-Vis spectra of Zn-TPc in toluene ($c = 5 \times 10^{-6}$ mol L^{-1}).

In order to gain more insights into the J-aggregation of Zn-TPc, molecular geometry optimization was performed in energy minimization mode. As shown in Fig. 10(a), the thiophene rings linked to the Pc core are tilted from the Pc core, and the dihedral angles between each thiophene ring and the Pc core are about 60°. Mckeown *et al.*[19] reported a series of Pcs with out-of-plane alkyl substituents, and found that these substituents served as a "picket-fence" to prevent the macrocycles from getting close to each other owing to mutual steric hindrance. The lowest energy conformation of Zn-TPc possesses similar characteristics to the "picket-fence" Pcs, which opposes aggregation.

In recent years, studies on several compounds[20] have revealed that a more planar conformation is favored in aggregates, even though the twist conformation is preferred in the isolated state. The J-aggregation behavior of Zn-TPc is thus thought to originate from its higher energy conformers. A possible mechanism is depicted in Fig. 10(a). Though the "picket-fence" conformation is dominant when Zn-TPc is molecularly dissolved in a good solvent, the rotation of thiophene rings generates other conformations with different coplanarization, in dynamic equilibrium. The coplanar conformers of Zn-TPc are theoretically advantageous to aggregate in terms of both electronic structure and steric hindrance. However, Zn-TPc can not assume a perfect coplanar conformation due to the consequent steric crowdedness, which precludes parallel face-to-face intermolecular interactions. In contrast, these coplanar conformers are arranged in head-to-tail direction, forming J-aggregates of Zn-TPc. This, in turn, induced more "picket fence" conformers to transform to coplanar conformers until new equilibria were established. Moreover, it is assumed that there are several different coplanar conformers that could J-aggregate, leading to various degrees of intermolecular π–π stackings with different bathochromic shifts of the Q-band absorption. This can explain why the J-band of Zn-TPc in chloroform was broad and not sharp and intense as previously reported.[5]

The different aggregation abilities between Ni-TPc and Zn-TPc can be explained by the intramolecular polarization between the phthalocyanine ring and its central metal. Abraham *et al.* investigated the π–π interaction of a series of porphyrins with different metal cores and found that the greater the intramolecular polarization between the porphyrin and the metal, the stronger is the π–π interaction between two porphyrins, thereby exhibiting larger tendency to aggregate.[21]

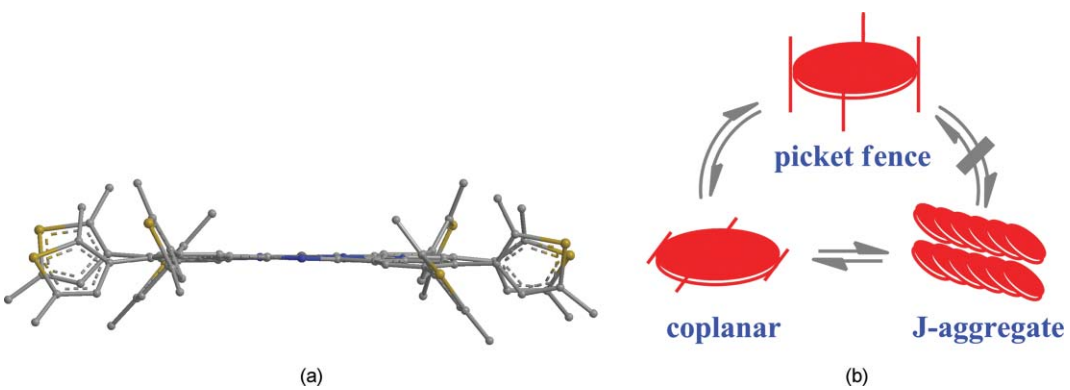

Fig. 10 (a) Computer optimized conformation of Zn-TPc by energy minimization method; (b) the mechanism for J-aggregation of Zn-TPc.

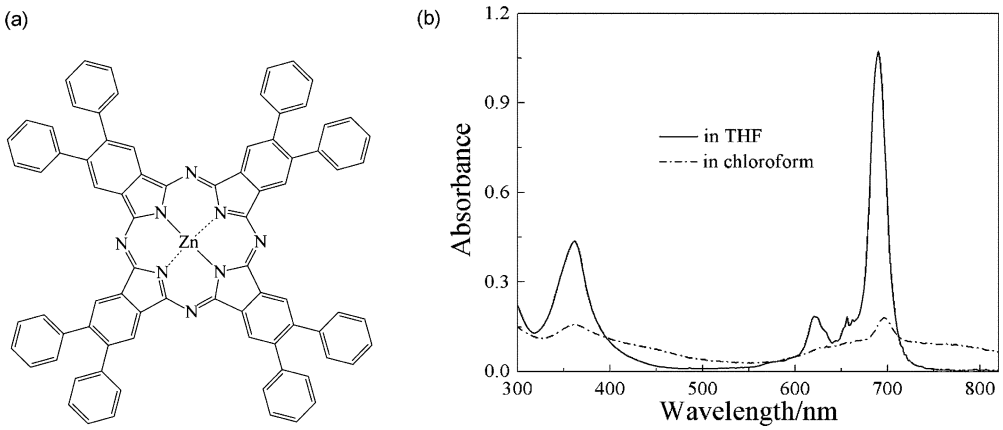

Fig. 11 (a) The chemical structure of Zn-PPc and (b) the UV-Vis spectra of Zn-PPc (5×10^{-6} mol L^{-1}) in THF and chloroform.

It is noteworthy that aforementioned "conformational planarization induced J-aggregation behavior" is not exclusive to Zn-TPc. We have observed that the octaphenyl-substituted zinc Pc (abbreviated as Zn-PPc), which possesses similar conformational characteristics to Zn-TPc (Fig. S8, ESI†), could also J-aggregate through the same mechanism. As an example, the solvent-dependent UV-Vis spectra of Zn-PPc (Fig. 11) demonstrated its J-aggregation properties. In THF, Zn-PPc exhibited an intense Q-band absorption at 698 nm, which is typical of monomer dispersion. When Zn-PPc was dissolved in chloroform, the absorption at 698 nm sharply decreased from 1.06 to 0.18. Meanwhile, a remarkably broadened and red shifted Q-band appeared, suggesting the formation of J-aggregates. The comparison between Fig. 11 and Fig. 3 revealed that Zn-PPc is more subject to J-aggregation than Zn-TPc. This result is in excellent agreement with the conformational analysis: the steric crowdedness involved in Zn-PPc is smaller than that in Zn-TPc. As a result, Zn-PPc forms coplanar conformers more easily. Besides, the π–π stacking ability of the phenyl substituent is larger than that of the thienyl substituent. These two reasons explain why ZnPPc showed much stronger J-aggregation tendency than Zn-TPc.

Conclusions

A novel family of thiophene-bearing phthalocyanines (M-TPcs) was synthesized, during which the key intermediate of these phthalocyanines was purified through a chemical approach. The synthetic route seems long and some intermediates were hard to purify, but in reality, the synthesis of target materials was facile thanks to the simplified separation procedures. In the lowest energy conformations of M-TPcs, the peripherally linked thiophene rings are tilted from the Pc core, which oppose aggregation theoretically. However, Zn-TPc tends to form J-aggregates through intermolecular π–π stacking and this tendency is especially remarkable in chloroform, whereas Ni-TPc and Cu-TPc showed excellent dispersibility. The unusual J-aggregation behavior of Zn-TPc was attributed its coplanar conformers. Octaphenyl-substituted zinc Pc (Zn-PPc) exhibited a similar J-aggregation behavior as Zn-TPc. We have thus discovered a new method to construct J-aggregates of Pcs. It is well-known that the J-aggregates of Pcs are highly desirable to maximize their optical properties. we believe this study will be helpful in both supramolecular chemistry and photonics.

Experimental

General remarks

Absorption spectra were measured by a diode array spectrophotometer HP8452A; IR spectra were obtained on a Nicolet Avatar 360 FT-IR spectroscopy; NMR spectra were recorded on a JOEL JNM-ECA300 spectrometer with TMS as the internal reference. Mass spectroscopy was recorded on a Bruker LC-MS/MS (ESQUIRE-LC) 1100; TOF-MS spectra were obtained with BEFLEX III. Elemental analyses were performed on a Carlo-Erba-1106 elementary analyzer. The fluorescence spectra were recorded with a Hitachi F-4500 fluorescence spectrophotometer. Melting points were measured using a XT4A microscopic melting point apparatus (Beijing Keyi Photo-electronic Corporation) and were uncorrected.

Except for the synthetic intermediates, reagents and solvents used in the present research are commercial products from Beijing Chemical Reagent Company. Solvents for spectroscopy measurements were refined by standard methods, while others were used as received. The solid film of Zn-TPc for UV-Vis study was prepared from a chloroform solution of Zn-TPc by spin-coating onto a glass plate and evaporation of the solvent.

Synthesis and charaterization

4,5-Dibromophthalic acid dimethyl ester (**1**), 2,5-dimethylthien-3-ylboronic acid and Zn-PPc were synthesized according to literature,[14,22,23] other steps are discussed below.

Compound 2

A mixture of 2,5-dimethylthien-3-ylboronic acid (3.91 g), 4,5-dibromophthalic acid dimethyl ester (2.96 g) and finely grounded dry potassium carbonate powder (9.17 g) was added into dioxane (30 mL) under argon flux. After being stirred for 15 min at room temperature, $Pd(PPh_3)_4$ (0.45 g) was added into the argon flow. The mixture was then heated to 90 °C for 9 h with TLC monitoring. After being cooled to room temperature, H_2O (50 mL)

and Et_2O (50 mL) were added, and the organic and aqueous phases were separated. The aqueous layer was then extracted twice with Et_2O. The combined organic phase was washed with NaOH solution (2 mol L^{-1}) and pure water in turn, dried over anhydride Na_2SO_4 and concentrated. Purification by column chromatography on silica gel (eluent: 1 : 3 petroleum–ethyl acetate) gave the crude product as a yellow dope. TLC showed that the R_f value of product is exactly the same as that of reagent **1**. ^{1}H NMR showed that the yellow dope is a mixture of compounds **1**, **2** and mono-substituted byproduct **8** with a molar ratio of 1 : 1.75 : 1.

Compound 3

The mixture obtained from the Suzuki cross-coupling reaction (3.80 g) was dissolved in THF (10 mL) and slowly added to a NaOH saturated mixed solution with water (10 mL) and methanol (50 mL). This was followed by stirring for 5 h at 40 °C. The white precipitate which formed was filtered off and washed with methanol. Then, it was dissolved in water and slowly acidified by dilute HCl (4 M) at 0 °C. The yellow precipitate (2.78 g) was collected and dried in vacuum. TLC showed that this reaction occurred quantitatively. The crude product was directly used in next step without further purifications.

Compound 4

The crude product obtained in the above step (2.78 g) was added to Ac_2O (12 mL) and the mixture was stirred at 80 °C for 2.5 h. AcOH generated in the reaction and excess Ac_2O were removed by azeotropic evaporation with toluene several times, and then dried in vacuum. TLC results showed that the starting materials completely disappeared. The yellow solid obtained was again directly used in the next step without any purification.

Compound 5

The product obtained above was placed in a round-bottomed flask containing 16 g urea under argon flow. The solid mixture was then heated to 140 °C, forming a clear, yellow melt. It was stirred for 15 min until bubbles ceased and then was allowed to cool to room temperature. Subsequently, water (100 mL) was added and the solid mixture was ultrasonically dispersed. The precipitate was collected and dried in vacuum. The reliability of this reaction was proved by TLC analysis. Without further purification, the precipitate was directly used in the next step.

Compound 6

The precipitate obtained in above reaction was dissolved in THF (20 mL) and mixed with concentrated ammonia (20 mL). This mixture was stirred for 48 h at room temperature and then allowed to stand for a few minutes. The organic phase was isolated and the aqueous layer extracted twice with THF (20 mL × 2). The organic phases were combined and concentrated under reduced pressure. The crude product (2.32 g) was dried in vacuum. TLC experiment showed that only 60% of the imides were converted to diamides. This crude was also directly used in next step without further purification.

Compound 7

The solid obtained in the above reaction (2.32 g) was dissolved in DMF (10 mL) and cooled to 0 °C under argon flow and a solution of $SOCl_2$ (9.5 mL) in DMF (7 mL) was slowly added. The solution was kept stirring for 2 h and then slowly poured into ice-water (40 mL). A faint yellow precipitate appeared and was collected. This solid was washed with saturated $NaHCO_3$ aqueous solution and pure water. The crude product (1.82 g) was dried in vacuum. TLC results showed that diamide was completely converted.

Purification of intermediate 7

The crude product (1.82 g) obtained in the reaction **6** → **7** and hydroquinone (3.00 g) was dissolved in *N*,*N*-dimethylformamide (10 ml). After being stirred for 15 min at room temperature, finely powdered dry potassium carbonate (2.20 g) was added. The mixture was kept stirring for 24 h at room temperature and then poured into 60 ml ice-water. After precipitation was complete, the pale yellow solid was filtered off and washed with water. The mixture of compound **11**, **12** and **7** was poured into an aqueous solution of sodium hydroxide and stirred for 5 min. The insoluble substance was collected and further purified by column chromatography over silica. The first band collected proved to be phthalonitrile **7** (0.72 g). The effectiveness of this approach was tested by various characterizations. ^{1}H NMR (300 MHz, $CDCl_3$, 25 °C): 2.03 (s, 6H, CH_3), 2.35 (s, 6H, CH_3), 6.25 (s, 2H, thiophene ring), 7.72 (s, 2H, benzene ring) ppm; ^{13}C NMR: 13.77, 15.11, 113.63, 115.59, 126.47, 134.24, 135.16, 135.82, 136.80, 141.94 ppm; IR/cm^{-1}: 3067.70, 2949.39, 2915.50, 2856.64, 2231.50 (CN), 1739.16, 1650.68, 1592.32, 1502.37, 1440.11, 1249.32, 1143.84, 830.97; ESI-MS: 371.07 ($M + Na^+$). Elemental analysis for $C_{20}H_{16}N_2S_2$: calc.: C 68.93, H 4.63, N 8.04; found: C 68.92, H 4.61, N 8.05%. Mp 121–122 °C.

The second band collected was proved to be pure intermediate **5**. ^{1}H NMR (300 MHz, $CDCl_3$, 25 °C), 2.05 (s, 6H), 2.44 (s, 6H), 6.27 (s, 2H), 7.80 (s, 2H), 7.85 (s, 1H) ppm; ^{13}C NMR: 13.81, 15.14, 126.00, 127.06, 130.90, 134.27, 135.90, 136.12, 167.98 ppm; IR/cm^{-1}: 3215.99, 3069.83, 2953.26, 2917.24, 2853.91, 11774.34, 1715.16, 1614.44, 1494,44, 1438.60, 1372.95, 1327.43, 834.53, 749.49; ESI-MS: 366.17 ($M - H^+$). Elemental analysis for $C_{20}H_{17}NO_2S_2$: calc.: C 65.37, H 4.66, N 3.81; found: C 65.34, H 4.62, N 3.82%. Mp 180–182 °C.

Zn-TPc

A mixture of phthalonitrile **7** (0.17 g), zinc acetate (37 mg), and DBU (80 mg) in 2-ethoxyethanol (8 ml) was refluxed for 3 h under argon flow. The resulting green suspension was cooled to ambient temperature and poured into 20 ml methanol. The precipitate was filtered off and washed with methanol. Finally, pure Zn-TPc (18 mg, yield: 10.1%) was obtained by chromatography on silica gel with 1 : 20 mixed solvent of ethyl acetate and chloroform as the eluent. MALDI-TOF: 1458.0 (calc: 1459.33); IR/cm^{-1}: 2913.83 (CH_3), 2852.25 (CH_3), 1644.05 (C═N), 1615.53 (Ben), 1495.37 (Ben), 1439.98 (Ben), 1347.64 (CH_3), 1094.04, 905.14 (Ben), 692.00 (Thio); UV-Vis (THF): λ_{max}/nm (log ε): 356 (4.75), 624 (4.51), 694 (5.24); ^{1}H NMR (TMS, 300 MHz, 5 : 1 mixed solvent of $CDCl_3$ and d_5-pyridine, 25 °C): 2.37 (s, 24H, CH_3), 2.51 (s, 24H, CH_3), 6.79 (s, 8H, thiophene ring), 9.57 (s, 8H, benzene ring) ppm. Elemental

analysis for $C_{80}H_{64}N_8S_8Zn$: calc.: C 65.84, H 4.42, N 7.68; found: C 65.82, H 4.43, N 7.65%.

Ni-TPc

Pure Ni-TPc (28 mg, 15.8% yield) was obtained through a similar procedure as in the synthesis of Zn-TPc with $NiCl_2$ used in place of $Zn(OAc)_2$ and the eluent changed to 1 : 3 petroleum–chloroform. MALDI-TOF: 1452.1 (calc: 1452.63); IR/cm^{-1}: 2915.57 (CH_3), 2850.08 (CH_3), 1652.51 (C═N), 1615.94 (Ben), 1496.23 (Ben), 1436.53 (Ben), 1375.56 (CH_3), 1099.36, 904.13 (Ben), 750.72 (Thio); UV-Vis (THF): λ_{max}/nm (log ε): 312 (4.81), 356 (4.75), 618 (4.46), 694 (5.16); ^{1}H NMR (TMS, 300 MHz, $CDCl_3$, 25 °C): 2.29 (s, 24H, CH_3), 2.48 (s, 24H. CH_3), 6.69 (s, 8H, thiophene ring), 9.29 (s, 8H, benzene ring) ppm. Elemental analysis for $C_{80}H_{64}N_8NiS_8$: calc.: C 65.15, H 4.44, N 7.71; found: C 65.17, H 4.42, N 7.73%.

Cu-TPc

Pure Ni-TPc (26 mg, 20.9% yield) was obtained through a similar procedure as in the synthesis of Zn-TPc with CuCl used in place of $Zn(OAc)_2$ and the eluent changed to chloroform. MALDI-TOF: 1457.2 (calc: 1457.48); IR/cm^{-1}: 2913.87 (CH_3), 2815.98 (CH_3), 1643.96 (C═N), 1611.83 (Ben), 1502.15 (Ben), 1436.41 (Ben), 1337 (CH_3), 1094, 900.28 (Ben), 693.91 (Thio); UV-Vis (THF): λ_{max}/nm (log ε): 350 (4.71), 622 (4.45), 692 (5.21). Elemental analysis for $C_{80}H_{64}CuN_8S_8$: calc. C 65.93, H 4.43, N 7.69; found: C 65.91, H 4.45, N 7.67%.

Acknowledgements

This work was supported by National Natural Science General Foundation of China (20773077), the Postdoctoral Science Funding (20090460297) and the National Key Fundamental Research Program (2007CB808000).

Notes and references

1 N. B. Mckeown, *Phthalocyanine Materials: Synthesis, Structure and Function*, Cambridge University Press, Cambridge, UK, 1998; K. M. Kadish, K. M. Smith, R. Guilard, *The Porphyrin Handbook*, Academic Press,San Diego, CA, 2003, vol 15: Phthalocyanines: Synthesis; H. Ali and J. E. Van Lier, *Chem. Rev.*, 1999, **99**, 2379; H. Yaku, T. Murashima, D. Miyoshi and N. Sugimoto, *Chem. Commun.*, 2010, **46**, 5740.
2 J. Rusanova, M. Pilkington and S. Decurtins, *Chem. Commun.*, 2002, 2236; Z. H. Chen, C. Zhong, Z. Zhang, Z. Y. Li, L. H. Niu, Y. J. Bin and F. S. Zhang, *J. Phys. Chem. B*, 2008, **112**, 7387; X. B. Leng, C-F. Choi, P-C. Lo and D. K. P. Ng, *Org. Lett.*, 2007, **9**, 231–234; T. Fukuda, I. Sugita and N. Kobayashi, *Chem. Commun.*, 2009, 2449.
3 K. M. Kadish, K. M. Smith, R. Guilard, *The Porphyrin Handbook,* Academic Press, San Diego, CA, 2003, Vol 17: Phthalocyanines: Properties and Materials.
4 M. Matsumoto, T. Nakazawa, R. Azumi, H. Tachibana, Y. Yaman- aka, H. Sakai and M. Abe, *J. Phys. Chem. B*, 2002, **106**, 11487.
5 K. Kameyama, M. Morisue, A. Satake and Y. Kobuke, *Angew. Chem., Int. Ed.*, 2005, **44**, 4763; J. L. Sessler, J. Jayawickramara-jah, A. Gouloumis, G. D. Pantos, T. Torres and D. M. Guldi, *Tetrahedron*, 2006, **62**, 2123–2131; X. Huang, F. Q. Zhao, Z. Y. Li, L. Huang, Y. W. Tang, F. Zhang and C-H. Tung, *Chem. Lett.*, 2007, **36**, 108; X Huang, F. Q. Zhao, Z. Y. Li, Y. W. Tang, F. S. Zhang and C-H. Tung, *Langmuir*, 2007, **23**, 5167; M. Morisue and Y. Kobuke, *Chem.–Eur. J.*, 2008, **14**, 4993–4700.
6 K. Adachi and H. Watarai, *J. Mater. Chem.*, 2005, **15**, 4701; K. Adachi, K. Chayama and H. Watarai, *Soft Matter*, 2005, **1**, 292; K. Adachi, K. Chayama and H. Watarai, *Langmuir*, 2006, **22**, 1630.
7 H. Isago, *Chem. Commun.*, 2003, 1864.
8 A. Mishra, C-Q. Ma and P. Bäuerle, *Chem. Rev.*, 2009, **109**, 1141.
9 For some recent examples, see: P. Gao, D. Berkmann, H. N. Tsao, X. L. Feng, V. Enkelmann, M. Baumgarten, W. Pisula and K. Müllen, *Adv. Mater.*, 2009, **21**, 213; T. Yasuda, H. Ooi, J. Morita, Y. Akama, K. Minoura, M. Funahashi, T. Shimomura and T. Kato, *Adv. Funct. Mater.*, 2009, **19**, 411; Y. Liu, Y. Wang, W. P. Wu, Y. Q. Liu, H. X. Xi, L. M. Wang, W. F. Qiu, K. Lu, C. Y. Du and G. Yu, *Adv. Mater.*, 2009, **19**, 772.
10 M. Irie, *Chem. Rev.*, 2000, **100**, 1685.
11 M. Q. He and F. X. Zhang, *J. Org. Chem.*, 2007, **72**, 442; X. C. Li, H. Sirringhaus, F. Garnier, A. B. Holmes, S. C. Moratti, N. Feeder, W. Clegg, S. J. Teat and R. H. Friend, *J. Am. Chem. Soc.*, 1998, **120**, 2206.
12 B. Z. Chen, M. Z. Wang, Y. Q. Wu and H. Tian, *Chem. Commun.*, 2002, 1060; H. Tian, B. Z. Chen, H. Y. Tu and K. Müllen, *Adv. Mater.*, 2002, **14**, 918; Q. F. Luo, B. Z. Chen, M. Z. Wang and H. Tian, *Adv. Funct. Mater.*, 2003, **13**, 233.
13 T. Muto, T. Temma, M. Kimura, K. Hanabusa and H. Shirai, *Chem. Commun.*, 2000, 1649.
14 C. C. Ko, W. M. Kwok, V. W. W. Yam and D. L. Phillips, *Chem.–Eur. J.*, 2006, **12**, 5840.
15 M. Gouterman, in *The Porphyrins*, ed. D. Dolphin, Academic Press, NY 1978, Vol. III, p. 1–165.
16 K. P. Seefeld, D. Mobius and H. Kuhn, *Helv. Chim. Acta*, 1977, **60**, 2608.
17 R. J. Abraham, F. Eivazi, H. Pearson and K. M. Smith, *J. Chem. Soc., Chem. Commun.*, 1976, 698.
18 G. M. Sander, M. van Dijk, A. Veldhuizen, H. C. Van der Plas, U. Hofstra and T. J. Schaafsma, *J. Org. Chem.*, 1988, **53**, 5272.
19 N. B. McKeown, M. Helliwell, B. M. Hassan, D. Hayhurst, H. Li, N. Thompson and S. J. Teat, *Chem.–Eur. J.*, 2007, **13**, 228.
20 M. Levitus, K. Schmieder, H. Ricks, K. D. Schimizu, U. H. F. Bunz and M. A. Garcia-Garibay, *J. Am. Chem. Soc.*, 2001, **123**, 4259; J. D. Luo, Z. L. Xie, J. W. Y. Lam, L. Cheng, H. Y. Chen, C. F. Qiu, H. S. Kwok, X. W. Zhan, Y. Q. Li, D. B. Zhu and B. Z. Tang, *Chem. Commun.*, 2001, 1740; B-K. An, S-K. Kwon, S-D Jung and S-Y. Park, *J. Am. Chem. Soc.*, 2002, **124**, 14410; K. N. Baker, A. V. Fratini, T. Resch, H. C. Knachel, W. W. Adams, E. P. Socci and B. L. Farmer, *Polymer*, 1993, **34**, 1571.
21 R. J. Abraham, F. Eivazi, H. Pearson and K. M. Smith, *J. Chem. Soc., Chem. Commun.*, 1976, 699.
22 Z. H. Chen, S. D. Dong, C. Zhong, Z. Zhang, L. H. Niu, Z. Y. Li and F. S. Zhang, *J. Photochem. Photobiol., A*, 2009, **206**, 213.
23 T. Sugimori, M. Torikata, J. Nojima, S. Tominaka, K. Tobikawa, M. Handa and K. Kasuga, *Inorg. Chem. Commun.*, 2002, **5**, 1031; S. A. Mikhalenko, L. A. Yagodina and E. A. Ink' yanets, *Zh. Obshch. Khim.*, 1976, **46**, 1598.